Journal of the Ceramic Society of Japan 112 [2] 65–69 (2004)

Paper

Positive Temperature Coefficient of Magnetization Characteristic for Composite Plastic-Bonded Magnet Composed of $Nd_2Fe_{14}B$ and $SrO{\cdot}6Fe_2O_3$

Yoshihiko MATSUYAMA, Hidehiko KOBAYASHI* and Takashi MITAMURA**

Kanex Co., 1710–36, Higashikata, Fukaya-shi, Saitama 366–0041
**Department of Applied Chemistry, Faculty of Engineering, Saitama University, 255, Shimoohkubo, Sakura-ku, Saitama-shi, Saitama 338–8570*
***Advanced Science Research Laboratory, Saitama Institute of Technology, 1690, Fusaiji, Okabe-machi, Ohsato-gun, Saitama 369–0293*

$Nd_2Fe_{14}B$ と $SrO{\cdot}6Fe_2O_3$ からなる複合プラスチックボンド磁石における磁化特性の正の温度係数

松山芳彦・小林秀彦*・三田村　孝**

（有）カネックス，366–0041 埼玉県深谷市東方 1710–36
*埼玉大学工学部応用化学科，338–8570 埼玉県さいたま市桜区下大久保 255
**埼玉工業大学先端科学研究所，369–0293 埼玉県大里郡岡部町普済寺 1690

Plastic-bonded magnets were prepared by magnetic field injection molding, using a mixture of $Nd_2Fe_{14}B$ and $SrO{\cdot}6Fe_2O_3$ pellets. The magnetic characteristics and temperature coefficients of these magnets were investigated. The hysteresis loop for the temperature change of the plastic-bonded magnet was measured. An important phenomenon was revealed pertaining to the physical properties of the magnetic material: under ordinary temperature conditions, the magnetic temperature coefficient of magnetic flux density and coercive force for the $Nd_2Fe_{14}B$ and $SrO{\cdot}6Fe_2O_3$ plastic-bonded magnet for the case of adequate $SrO{\cdot}6Fe_2O_3$ content attained a positive value at a $SrO{\cdot}6Fe_2O_3$ content ranging from about 20 to 60 mass% at 297–323 K, and from around 18 to 43 mass% at 323–373 K. Moreover, it was proven that the temperature coefficients of the magnetic flux density at operating points of permeance coefficients $P_c(B/H) = 1$ and 2 could be controlled from 0 to 0.22%/K at 297–323 K and from 0 to 0.1%/K at 323–373 K, respectively. [Received April 9, 2003; Accepted November 27, 2003]

Key-words: *Neodymium iron boron, Strontium ferrite, Magnetic field injection molding, Positive temperature coefficient, Permeance coefficient*

1. Introduction

The temperature coefficient of magnetic flux density for a permanent magnet appears to assume a positive or negative value due to heat process when the permeance coefficient approaches a small or large value. The phenomenon is well-established in magnetic materials such as Alnico alloy[1] and strontium ferrite ($SrO{\cdot}6Fe_2O_3$).[2] The temperature coefficient of the residual magnetic flux density Br of $SrO{\cdot}6Fe_2O_3$ is reduced to −0.2%/K, while the temperature coefficient of coercive force H_{c_B} is increased to 0.2–0.5%/K. Thus, permanent magnets have been designed by choosing an operating point where the temperature coefficient value of the magnetic flux density for the permeance coefficient is approximately zero.

It is well-known that the temperature coefficient of magnetic flux density decreases with increasing temperature to about $-0.11 \sim -0.13$%/K in the case of neodymium iron boron ($Nd_2Fe_{14}B$).[3),4)] The temperature coefficient of the magnetic flux density for the $Nd_2Fe_{14}B$ has a negative value regardless of the permeance coefficient value. The temperature dependence of the demagnetization curve of $Nd_2Fe_{14}B$ is also well-established. Thus, the operating point on the demagnetization curve of $Nd_2Fe_{14}B$ will take on a negative value with increasing temperature, even when one attempts to vary the permeance coefficient.

In this study, the $Nd_2Fe_{14}B$ and $SrO{\cdot}6Fe_2O_3$ pellets were formed separately, and the magnetization curve and the temperature coefficient of the magnetic flux density were investigated using a plastic-bonded $Nd_2Fe_{14}B$–$SrO{\cdot}6Fe_2O_3$ pellet of varying composition. The plastic-bonded specimens were prepared by magnetic field injection molding. The $Nd_2Fe_{14}B$ plastic-bonded magnet was found to have a positive temperature coefficient of the magnetic flux density in the appropriate range of $SrO{\cdot}6Fe_2O_3$ content.

2. Experimental

2.1 Preparation of $Nd_2Fe_{14}B$–$SrO{\cdot}6Fe_2O_3$ magnetic pellets

Commercial neodymium iron boron ($Nd_2Fe_{14}B$)[4] (Magnequench International Inc.) and strontium ferrite ($SrO{\cdot}6Fe_2O_3$) (Toda Kogyo Co.) were used. Crushed ribbons of the $Nd_2Fe_{14}B$ are isotropic and polycrystalline magnetic ribbons, while the $SrO{\cdot}6Fe_2O_3$ is an anisotropic fine magnetic powder. Characteristics of these powders used as the starting materials of $Nd_2Fe_{14}B$–$SrO{\cdot}6Fe_2O_3$ pellets are shown in **Table 1**.

First, $Nd_2Fe_{14}B$ which seems to react with $SrO{\cdot}6Fe_2O_3$ and $SrO{\cdot}6Fe_2O_3$ pellets were prepared separately. The anisotropic $SrO{\cdot}6Fe_2O_3$ pellets were formed by compressing a mixture of fine $SrO{\cdot}6Fe_2O_3$ powder, 12-nylon (12-Degeneracy coalescence of the amino dodecanoic acid) as thermosetting resin, lubricants (calci-

Table 1. Characteristics of Powders Used as the Starting Materials of $Nd_2Fe_{14}B$–$SrO{\cdot}6Fe_2O_3$ Pellets

$Nd_2Fe_{14}B$

Br (T)	Hc_B (kA/m)	Hc_J (kA/m)	mean particle size (μm)	mean aspect ratio
0.8	398.1	716.6	200	1:5

$SrO{\cdot}6Fe_2O_3$

Br (T)	Hc_B (kA/m)	Hc_J (kA/m)	mean particle size (μm)	mean aspect ratio
0.289	180.0	212.6	1.50	1:1.2

Table 2. Additive Compounds and Their Relative Proportions for the Preparation of $Nd_2Fe_{14}B$ and $SrO{\cdot}6Fe_2O_3$ Pellets

$Nd_2Fe_{14}B$ pellet

Compound	$Nd_2Fe_{14}B$	SCA	12-nylon	sulfonamide	calcium stearate
Proportion	87.75 mass%	1.0 mass%	11 mass%	0.2 mass%	0.05 mass%

$SrO{\cdot}6Fe_2O_3$ pellet

Compound	$SrO{\cdot}6Fe_2O_3$	SCA	12-nylon	sulfonamide	calcium stearate
Proportion	87.75 mass%	1.0 mass%	11 mass%	0.2 mass%	0.05 mass%

um stearate) and sulfonamide plasticizers (*N*-butylbenzene sulfonamide), and a silane coupling agent (SCA, *N*-(2-aminoethyl)3-aminopropyltrimethoxysilane). SCA served to strengthen the bond between the magnetic powders and thermosetting resin. The isotropic $Nd_2Fe_{14}B$ pellets with shape crushed ribbons were prepared in a similar method, after the surface of the $Nd_2Fe_{14}B$ crushed ribbons was coated with a small amount of silane coupling agent. The proportions of the various components are shown in **Table 2**.

Next, the pellets were mixed at one of the following $Nd_2Fe_{14}B$ to $SrO{\cdot}6Fe_2O_3$ ratios: 0/100, 30/70, 50/50, 70/30 and 100/0 by mass (hereafter referred to as samples A, B, C, D and E, respectively). The pellet mixture was then heated to 553 K and injection molded into a $\phi 20\times 10$ mm metal mold maintained at 373 K. The resultant pellet was magnetized along the axial direction of the anisotropic magnetic particles, yielding a plastic-bonded magnet pellet. The *B–H* curve for this pellet was obtained.

2.2 Measurement of magnetic characteristics

Magnetic characteristics of the *B–H* curve were determined using the setup (Riken Res. Electron Co.) schematized in **Fig. 1**. The temperature of the specimen ($\phi 20\times 10$ mm, axially anisotropic) was varied at 297–323, 323–373 and 373–413 K (thermocouple was used to monitor the temperature) during the measurements order to determine the effect of temperature. The magnetic field strength used in the magnetization experiment was 796 kA/m.

An instrument equipped with a superconductor (NbTi) enabled the generation of a large current used in measuring magnetic characteristics at 260 and 290 K as shown in **Fig. 2**. Pulse magnetization for measuring device of pulse coil was fixed in the multilayer roll line coil in the epoxy resin. The specimen ($3\times 3\times 3$ mm for perfect magnetic saturation) was cooled from 260 to 290 K using dry ice. The magnetic field strength of magnetization was 7960 kA/m. A sine pulse wave (1 cycle/18 s) was employed in the measurements. Since $SrO{\cdot}6Fe_2O_3$ was magnetically saturated at 796 kA/m but $Nd_2Fe_{14}B$ was not, a magnetic field of 7960 kA/m was applied to confirm the data obtained at 796 kA/m.

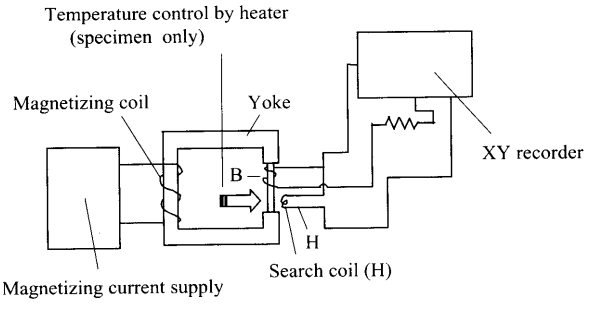

Fig. 1. Automatic equipment for measuring hysteresis loop by DC drive.

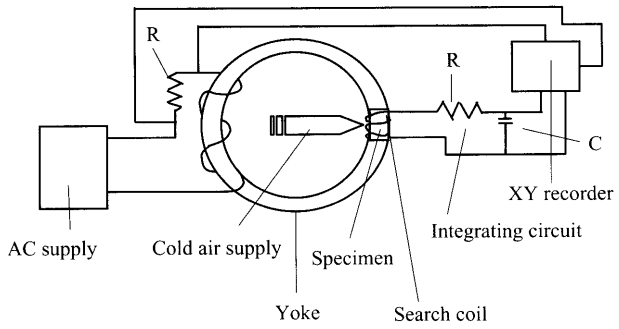

Fig. 2. System for hysteresis loop measurement by a pulse magnetization measuring device incorporating a superconductor for the generation of large current.

3. Results and discussion

3.1 Magnetic characteristics of plastic-bonded $Nd_2Fe_{14}B$–$SrO{\cdot}6Fe_2O_3$ magnet

The magnetic flux density, the size of the magnetization and the value of coercive force have been discussed generally. However, the specimens were examined based on the change in the hysteresis loop due to temperature change, because it is important industrially that the change in the magnetic flux density becomes zero or positive as the temperature rises.

The automatic magnetism equipment was used to obtain the magnetic hysteresis loop for specimens A, B, C, D and E over the 297–323, 323–373 and 373–413 K temperature range, under a magnetic field of 796 kA/m. Over the 260–290 K temperature range, measurements were carried out under a magnetic field of 7960 kA/m instead, using the equipment with the superconductor shown in Fig. 2. Though the saturation magnetic flux values differed greatly, the temperature coefficients of the magnetic flux density were virtually identical despite the large difference in the magnetic field used (**Table 3**). The error in the data was quite significant in the case of the large magnetic field. Thus, these results were analyzed on the basis of the measurements taken over the 297–413 K range under 796 kA/m. *J–H* curves of five kinds of $Nd_2Fe_{14}B$–$SrO{\cdot}6Fe_2O_3$ magnets are shown in **Fig. 3**. Technical terms such as Br and permeance coefficient of *B–H* demagnetizing curves are illustrated in **Fig. 4**.

The measurements of the temperature coefficient of magnetic flux density were carried out on the basis of the *B–H* demagnetizing curves. The relationship between the temperature coefficient of residual magnetic flux density Br and $SrO{\cdot}6Fe_2O_3$ content is shown in **Fig. 5** for three temperature ranges: 297–323, 323–373 and 373–413 K. The temperature coefficient of the magnetic flux density for the $SrO{\cdot}6Fe_2O_3$-free $Nd_2Fe_{14}B$ magnet was negative.

Table 3. Temperature Coefficients of Magnetic Flux Density and Coercive Force for Specimens (B, C, D and E) Obtained under a Magnetic Field of 7960 kA/m

Specimen	Temp. (K)	Br (T)	Temp.coef. (%/K)	Hc_B (kA/m)	Temp.coef. (%/K)	Hc_J (kA/m)	Temp.coef. (%/K)
B	290	0.234	−0.098	183.1	0.318	509.6	0
	260	0.241		167.2		509.6	
C	290	0.201	−0.221	159.2	0	398.1	0
	260	0.215		159.2		398.1	
D	290	0.188	−0.180	151.3	0.090	414.0	−0.123
	260	0.198		147.3		429.9	
E	290	0.161	−0.174	135.4	−0.351	414.0	0.355
	260	0.170		139.7		374.2	

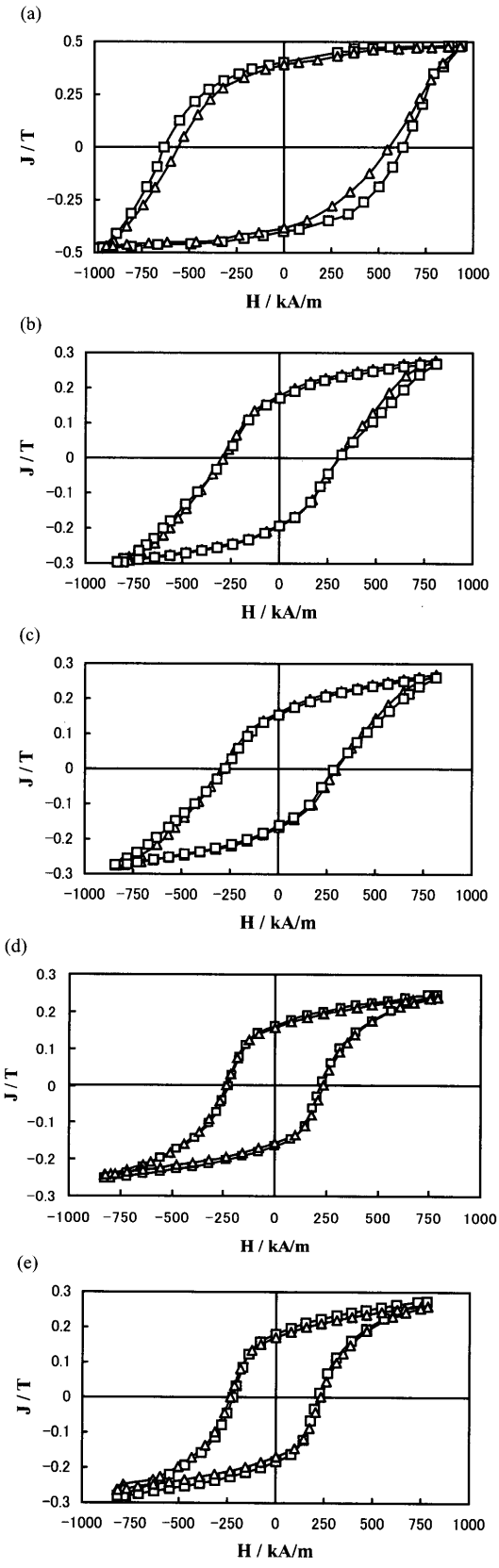

Fig. 3. *J–H* loops of composite $Nd_2Fe_{14}B$–$SrO{\cdot}6Fe_2O_3$ magnets.
□ 297–323 K, △ 323–373 K.
(a) free $SrO{\cdot}6Fe_2O_3$–100 mass% $Nd_2Fe_{14}B$ magnet,
(b) 30 mass% $SrO{\cdot}6Fe_2O_3$–70 mass% $Nd_2Fe_{14}B$ magnet,
(c) 50 mass% $SrO{\cdot}6Fe_2O_3$–50 mass% $Nd_2Fe_{14}B$ magnet,
(d) 70 mass% $SrO{\cdot}6Fe_2O_3$–30 mass% $Nd_2Fe_{14}B$ magnet,
(e) 100 mass% $SrO{\cdot}6Fe_2O_3$–free $Nd_2Fe_{14}B$ magnet.

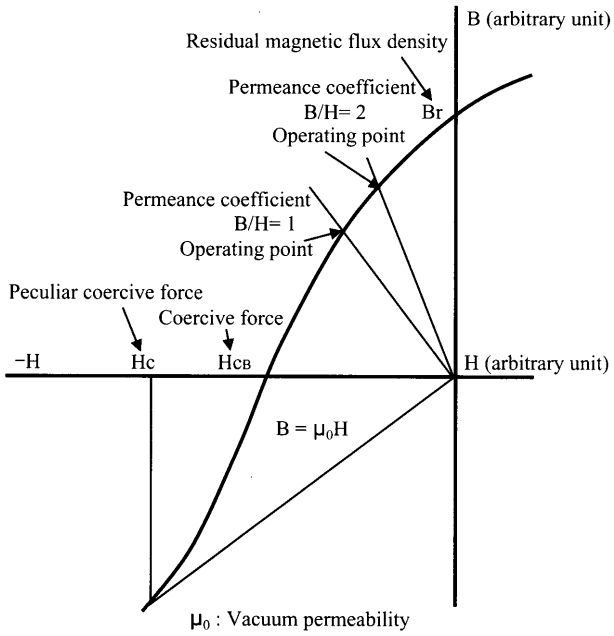

Fig. 4. Description of general technical terms concerning the demagnetization curve of the *B–H* curve.

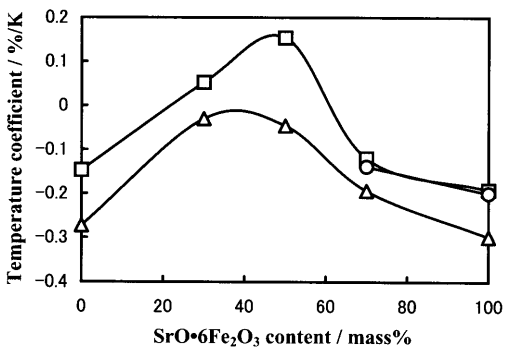

Fig. 5. Effect of $SrO{\cdot}6Fe_2O_3$ addition on the temperature coefficient of residual magnetic flux density Br for a $Nd_2Fe_{14}B$ magnet.
□ 297–323 K, △ 323–373 K, ○ 373–413 K.

The temperature coefficient was zero at about 20 and 60 mass% $SrO{\cdot}6Fe_2O_3$ at 297–323 K and positive between about 20 and 60 mass% $SrO{\cdot}6Fe_2O_3$. The positive temperature coefficient of the magnetic flux density reached its maximum at about 50 mass% $SrO{\cdot}6Fe_2O_3$ (specimen C).

In general, the current value of motor and actuator magnets decreases remarkably with rising temperature, since the resistance value of copper wire increases. Accordingly, the increase of the magnetic flux density is indispensable. As a result, the development of permanent magnet, which the temperature coefficient of magnetic flux density is zero or positive, is anticipated industrially. The magnets of these devices[4),5)] are generally used at the operating point of permeance coefficient $P_c(B/H)$[6)] = 1 or 2 on the general demagnetization curve shown in Fig. 3. Magnetic characteristics derived from the *J–H* loops of composite $Nd_2Fe_{14}B$–$SrO{\cdot}6Fe_2O_3$ magnets measured at ordinary temperature (297–323 K) (refer to Figs. 3(b), (c) and (d)) are shown in **Table 4** for the design of the devices described above, where (BH)max and J_S are the maximum energy product and the saturation magnetic flux density, respectively.

Based on the above results, the temperature coefficients of the

Table 4. Characteristics Derived from *J–H* Loops of $Nd_2Fe_{14}B$–$SrO{\cdot}6Fe_2O_3$ Magnets Measured at 297–323 K

Magnet	Br (T)	Hc_B (kA/m)	Hc_J (kA/m)	(BH)max (kJ/m^3)	J_S (T)
30 mass% $SrO{\cdot}6Fe_2O_3$ 70 mass% $Nd_2Fe_{14}B$	0.160	113.0	243	5.41	0.29
50 mass% $SrO{\cdot}6Fe_2O_3$ 50 mass% $Nd_2Fe_{14}B$	0.155	103.5	275	4.46	0.24
70 mass% $SrO{\cdot}6Fe_2O_3$ 30 mass% $Nd_2Fe_{14}B$	0.180	107.5	300	4.50	0.25

magnetic flux density at the operating point of permeance coefficient $P_c(B/H) = 1$ at 297–323, 323–373 and 373–413 K for the $Nd_2Fe_{14}B$ magnet as a function of $SrO{\cdot}6Fe_2O_3$ content are shown in **Fig. 6**. The temperature coefficient of the magnetic flux density was positive between about 20 and 60 mass% $SrO{\cdot}6Fe_2O_3$ at 297–323 K, and positive between about 18 and 43 mass% $SrO{\cdot}6Fe_2O_3$ at 323–373 K. The maximum values obtained from the figure were about 0.23 and 0.1%/K at approximately 47 mass% $SrO{\cdot}6Fe_2O_3$ at 297–323 K and 30 mass% $SrO{\cdot}6Fe_2O_3$ at 323–373 K, respectively. The temperature coefficients of the magnetic flux density at the operating point of permeance coefficient $P_c(B/H) = 2$ over these temperature ranges are shown in **Fig. 7**. The change in temperature coefficients of the magnetic flux density was similar to that of $P_c(B/H) = 1$. The temperature coefficient was positive between about 18 and 60 mass% $SrO{\cdot}6Fe_2O_3$ at 297–323 K and between about 20 and 42 mass% $SrO{\cdot}6Fe_2O_3$ at 323–373 K. The

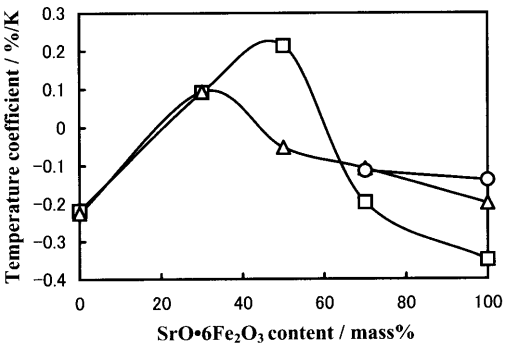

Fig. 6. Effect of $SrO{\cdot}6Fe_2O_3$ addition on the temperature coefficient of magnetic flux density at operating point of permeance coefficient $P_c(B/H) = 1$ for a $Nd_2Fe_{14}B$ magnet.

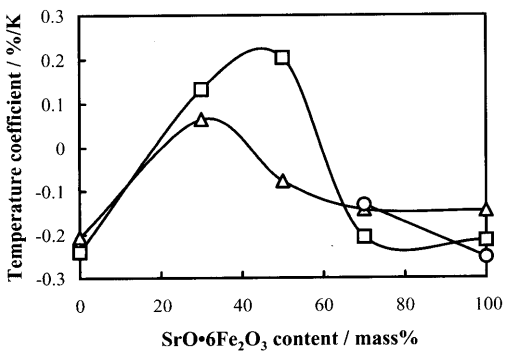

Fig. 7. Effect of $SrO{\cdot}6Fe_2O_3$ addition on the temperature coefficient of magnetic flux density at operating point of permeance coefficient $P_c(B/H) = 2$ for a $Nd_2Fe_{14}B$ magnet.
□ 297–323 K, △ 323–373 K, ○ 373–413 K.

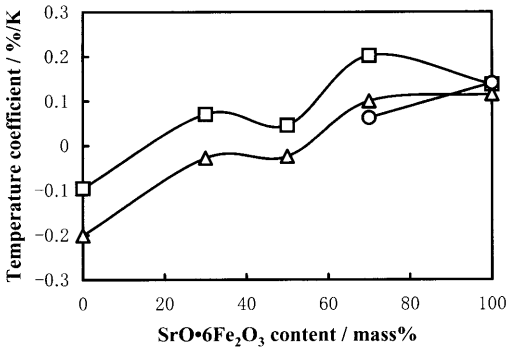

Fig. 8. Effect of $SrO{\cdot}6Fe_2O_3$ addition on the temperature coefficient of coercive force H_{c_B} for a $Nd_2Fe_{14}B$ magnet.
□ 297–323 K, △ 323–373 K, ○ 373–413 K.

maximum values obtained from the figure were about 0.23 and 0.07%/K at approximately 44.6 mass% $SrO{\cdot}6Fe_2O_3$ at 297–323 K and 32 mass% $SrO{\cdot}6Fe_2O_3$ at 323–373 K, respectively. These results indicate that the temperature coefficient of the magnetic flux density for the $Nd_2Fe_{14}B$ magnet can be controlled and made to be positive or equal to zero by the appropriate choice of $SrO{\cdot}6Fe_2O_3$ content between *RT* and 373 K.

The temperature coefficient measurements of the coercive force H_{c_B} for specimens A, B, C, D and E at 297–323, 323–373 and 373–413 K are shown in **Fig. 8**. The temperature coefficient of the coercive force for the $Nd_2Fe_{14}B$ magnet containing no $SrO{\cdot}6Fe_2O_3$ was negative, but increased with $SrO{\cdot}6Fe_2O_3$ content and became positive above approximately 16 mass% at 297–323 K and 53 mass% at 323–373 K.

3.2 Formation mechanism of $Nd_2Fe_{14}B$ magnet with positive temperature coefficient

Residual magnetic flux density Br and coercive force H_{c_B} on the demagnetization curves of isotropic $Nd_2Fe_{14}B$ crushed ribbons decrease with increasing temperature, and a negative temperature coefficient of the magnetic flux density and the coercive force is observed on all demagnetization curves. On the other hand, the temperature coefficient of residual magnetic flux density Br on the demagnetization curve of anisotropic $SrO{\cdot}6Fe_2O_3$ is negative, while the temperature coefficient in coercive force H_{c_B} is positive. However, it became clear that the unique phenomenon concerning the temperature coefficient of the magnetic flux density emerged upon mixing $Nd_2Fe_{14}B$ and $SrO{\cdot}6Fe_2O_3$ at the appropriate proportion.

Micrographs of the microstructure of specimen C as measured by electron prove microanalyzer (EPMA; JXA 8900R, JEOL), exhibiting a positive temperature coefficient of the magnetic flux density at 297–323 K, are shown in **Fig. 9**. It was confirmed by XRD (RINT 2000, Rigaku) and fluorescent X-ray analyzer (ZSX, Rigaku) that the Nd–Fe–B and Sr–Fe–O elements shown in Fig. 9 are $Nd_2Fe_{14}B$ and $SrO{\cdot}6Fe_2O_3$, respectively.

$Nd_2Fe_{14}B$ is crystallographically isotropic. Since the $Nd_2Fe_{14}B$ crushed ribbons were processed by quenching, they appear to become isotropic crystallite aggregate. These crushed ribbons have shape anisotropy, as they have a magnetic easy axis in the oblong direction. However, after the orientation magnetic field was removed, an equilibrium appears to have been reached through the formation of a minor closed magnetic circuit,[7] which is appropriate for the size of the $SrO{\cdot}6Fe_2O_3$ fine particle, as a result of the large difference in H_{c_B} between the $Nd_2Fe_{14}B$ (H_{c_B}: 501 kA/m) and $SrO{\cdot}6Fe_2O_3$ (H_{c_B}: 127 kA/m) and the inversion of a number of the isotropic $Nd_2Fe_{14}B$ crystallite bodies. As it can be seen from Figs. 3(b) and (c), the *J–H* curves increased rapidly near

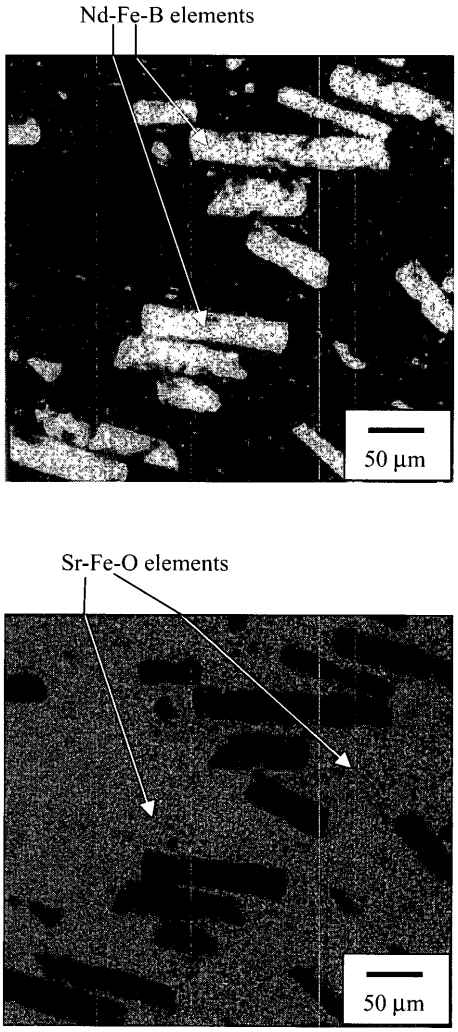

Fig. 9. Micrographs of the elements for $Nd_2Fe_{14}B$ and $SrO{\cdot}6Fe_2O_3$ measured by EPMA for specimen C.

the saturation magnetic flux density in the temperature range of 323–373 K. Therefore, it is considered that the minor closed magnetic circuits are opened so that all $Nd_2Fe_{14}B$ and $SrO{\cdot}6Fe_2O_3$ magnetic domains may turn to the direction of magnetic field. Consequently, the magnetic flux density for Br of $Nd_2Fe_{14}B$ is reduced. The Br and H_{c_B} of the demagnetization curve of the $Nd_2Fe_{14}B$ decrease with increasing temperature. On the other hand, the Br decreases and the H_{c_B} of $SrO{\cdot}6Fe_2O_3$ increases. As a result, the equilibrium breaks down with increasing temperature, and the magnetic flux density of $Nd_2Fe_{14}B$ appears to increase.

Thus, the temperature coefficient of the magnetic flux density for the $Nd_2Fe_{14}B$ magnet becomes zero at about 20 mass% $SrO{\cdot}6Fe_2O_3$ and positive upon further addition of $SrO{\cdot}6Fe_2O_3$ at 297–323 K, reaching its maximum positive value at about 50 mass% $SrO{\cdot}6Fe_2O_3$. With increasing $SrO{\cdot}6Fe_2O_3$ content, the minor closed magnetic circuits become saturated since the quantity of $Nd_2Fe_{14}B$ decreases when $SrO{\cdot}6Fe_2O_3$ is increased; the temperature coefficient of the magnetic flux density becomes zero at about 60 mass% $SrO{\cdot}6Fe_2O_3$. At higher $SrO{\cdot}6Fe_2O_3$ contents, the temperature coefficient of the magnetic flux density approaches that of $SrO{\cdot}6Fe_2O_3$.

A similar tendency is observed even in the temperature range of 323–373 K. However, minor closed magnetic circuits can be formed whereby the magnetic flux density drops with increasing temperature, and the absolute value of the temperature coefficient of the magnetic flux density decreases.

The mechanism detailed above explains how the temperature coefficient of the magnetic flux density becomes zero or attains a positive value at the operating points of permeance coefficients $P_c(B/H) = 1$ and 2. Moreover, the magnet's coercive force H_{c_B} retains the essential positive temperature coefficient.

The magnetic flux density of the composite plastic-bonded magnet composed of $Nd_2Fe_{14}B$ and $SrO{\cdot}6Fe_2O_3$ in the present paper was approximated as the magnetic flux density of $SrO{\cdot}6Fe_2O_3$. Consequently, we pursued by the attention on not the meaning in which the magnetic flux density is improved, but rather the cause of the temperature dependency of the magnetization for the composite plastic-bonded magnet to the existence of the unique behavior.

4. Conclusion

Plastic-bonded magnets were fabricated from $Nd_2Fe_{14}B$ and $SrO{\cdot}6Fe_2O_3$ pellets, and their temperature coefficients were investigated. The following results were obtained:

(1) At the operating point of permeance coefficient $P_c(B/H) = 1$, the temperature coefficients of the magnetic flux density for the magnet were positive between about 20 and 60 mass% $SrO{\cdot}6Fe_2O_3$ at 297–323 K, and between about 18 and 43 mass% $SrO{\cdot}6Fe_2O_3$ at 323–373 K. The maximum values obtained from the figure were about 0.23 and 0.1%/K at approximately 47 mass% $SrO{\cdot}6Fe_2O_3$ at 297–323 K and approximately 30 mass% $SrO{\cdot}6Fe_2O_3$ at 323–373 K, respectively.

(2) At the operating point of permeance coefficient $P_c(B/H) = 2$, the temperature coefficients of the magnetic flux density for the magnet were positive between about 18 and 60 mass% $SrO{\cdot}6Fe_2O_3$ at 297–323 K, and between about 20 and 42 mass% $SrO{\cdot}6Fe_2O_3$ at 323–373 K. The maximum values obtained from the figure were about 0.23 and 0.07%/K at approximately 44.6 mass% $SrO{\cdot}6Fe_2O_3$ at 297–323 K and 32 mass% $SrO{\cdot}6Fe_2O_3$ at 323–373 K, respectively.

(3) Upon the addition of anisotropic $SrO{\cdot}6Fe_2O_3$ to isotropic $Nd_2Fe_{14}B$, the temperature coefficient of the magnetic flux density at the operating points of permeance coefficients $P_c(B/H) = 1$ and 2 on the demagnetization curve of $Nd_2Fe_{14}B$ becomes zero or positive in proportion to the amount of $SrO{\cdot}6Fe_2O_3$ added. Thus, the temperature coefficient of the magnetic flux density for the $Nd_2Fe_{14}B$ magnet is readily controlled in the ordinary temperature range from 297 to 323 K.

Acknowledgements The support provided by the High Technological Research Center of Saitama Institute of Technology in carrying out this work is gratefully acknowledged. The authors would like to express our appreciation to Prof. Noboru Miura, the Institute for Solid State Physics, Tokyo University, for measuring of the pulse magnetization and discussion.

References

1) Parker, R. J. and Studders, R. J., "Permanent Magnets and Their Application," John Wiley & Sons (1962) pp. 339–350.
2) Lommel, J. M., *J. Appl. Phys.*, Vol. 40, pp. 1294–1296 (1969).
3) Nozawa, Y., Iwasaki, K., Tanigawa, S., Tokunaga, M. and Harada, H., *J. Appl. Phys.*, Vol. 64, pp. 5285–5289 (1988).
4) Panchanathan, V., 16th IREM (2000) pp. 431–445.
5) Parker, R. J. and Studders, R. J., "Permanent Magnets and Their Application," John Wiley & Sons (1962) pp. 210–286.
6) Parker, R. J. and Studders, R. J., "Permanent Magnets and Their Application," John Wiley & Sons (1962) pp. 163–176.
7) Brenner, R. and Pfeifer, F., *Frequenz*, Vol. 15, pp. 87–89 (1961).